



On fully symmetric implicit closure approximations for fiber orientation tensors

Tobias Karl^{a,b,*}, Matti Schneider^a, Thomas Böhlke^a

^a Institute of Engineering Mechanics, Chair for Continuum Mechanics, Karlsruhe Institute of Technology (KIT), Kaiserstraße 10, 76131 Karlsruhe, Germany

^b Institute of Fluid Mechanics, Karlsruhe Institute of Technology (KIT), Kaiserstraße 10, 76131 Karlsruhe, Germany

ARTICLE INFO

Keywords:

Fiber orientation
Composites
Closure approximation
Folgar–Tucker equation
Anisotropy
Homogenization

ABSTRACT

A novel closure approximation method for fiber orientation tensors is proposed namely the fully symmetric implicit closure. Besides the full index symmetry, implicitly formulated closures based on the contraction condition fulfill the trace condition and the trace-preserving property of the Folgar–Tucker equation. As a first example, the fully symmetric implicit quadratic closure is considered as a simple modification of a recently proposed symmetric quadratic closure. It is shown that this closure can be realized by a fiber orientation distribution function. Secondly, the fully symmetric implicit hybrid closure is proposed as a counterexample of a closure not being based on an orientation distribution function. Both closures are compared against classical approximations in view of orientation evolution in a simple shear flow. Furthermore, the capability of predicting the effective viscous and elastic behavior of fiber suspensions and solid composites is investigated for a given fiber orientation state. The results show that the proposed implicit closures can be used to approximate the maximum entropy closure. Thereby, both the quadratic and the hybrid approach alleviate the high computational burden of the maximum entropy closure, as their evaluation requires solving a one-dimensional problem only. In addition, the predicted effective behavior based on the implicit closures shows an overall good agreement with predictions based on measured orientation data.

1. Introduction

1.1. Motivation and state of the art

In the framework of lightweight composites, considering microstructural information is essential for industrial applications in view of predicting anisotropic properties. For the special case of fiber reinforced composites, orientation tensors [1,2] are widely used as an efficient way of describing strongly heterogeneous and anisotropic microstructures. Typically only the second-order fiber orientation tensor is known as a result of mold-filling simulations. In order to perform these mold-filling simulations, the fourth-order orientation tensor has to be known for solving the corresponding evolution equation for the second-order orientation tensor [2,3]. Also the approximation of the effective viscous and elastic behavior [4] requires the fourth-order orientation tensor in view of homogenization by using orientation averaging [2]. In this context, closure methods for fiber orientation tensors are used to approximate the fourth-order orientation tensor as a function of the second-order orientation tensor. Designing an accurate closure under consideration of all necessary algebraic properties is a non-trivial task.

A comprehensive listing of various closure approximations is given in Breuer et al. [5] and in the recent publication of Al-Qudsi et al. [6]. A novel orthotropic fitted closure was proposed by Al-Qudsi et al. [6] and different well known closure approximations were compared against each other in terms of Young's moduli and experimental investigations. Reasonable elasticity approximations were achieved except for the so called 'simple closures': the linear closure [2,7,8], the quadratic closure [9] and the hybrid closure [2,8]. Han and Im [10] developed an improved hybrid closure. In addition, Petty et al. [11] proposed a generalized hybrid closure approach in order to address the lack of full index symmetry of the common hybrid closure. In this context, Karl et al. [12] improved the quadratic closure approximation by symmetrization and derived two versions of this symmetric quadratic closure, one for orientation evolution prediction and the other one for estimating effective viscous and elastic behavior. Based on the angular central Gaussian distribution (ACG) [13], Montgomery-Smith et al. [14,15] introduced the fast exact closure for the Folgar–Tucker equation [2,16] without fiber–fiber interaction. Regarding the generation of straight short-fiber microstructures, the ACG closure was used

* Corresponding author at: Institute of Engineering Mechanics, Chair for Continuum Mechanics, Karlsruhe Institute of Technology (KIT), Kaiserstraße 10, 76131 Karlsruhe, Germany.

E-mail address: tobias.karl@kit.edu (T. Karl).

<https://doi.org/10.1016/j.jnnfm.2023.105049>

Received 21 November 2022; Received in revised form 12 April 2023; Accepted 14 April 2023

Available online 23 April 2023

0377-0257/© 2023 The Authors. Published by Elsevier B.V. This is an open access article under the CC BY license (<http://creativecommons.org/licenses/by/4.0/>).

by Schneider [17] and for the generation of curved fiber microstructures by Schneider [18], respectively. Köbler et al. [19] and Bertóti et al. [20] used the algorithm of Schneider [17] to generate short-fiber microstructures as a basis of full-field simulations. Regarding an orientation-adapted integration scheme on the unit sphere, Goldberg et al. [21] also used the ACG closure. Nabergoj et al. [22] used an ellipsoid function in view of a function-based reconstruction method for the orientation distribution function only dependent on the second-order fiber orientation tensor. This function-based approach circumvents several problems of the series-based approach, namely negative values and sharp orientation distributions [5,22]. Based on the proposed function-based approach, a closure of orthotropic nature for the fourth-order orientation tensor was derived. Recently, Ogierman [23] proposed a generic closure approximation based on an optimization procedure. This closure led to precise results and offered the distribution of the elastic constants, but appeared to be rather inefficient compared to more common closures. Regarding the admissible parameter space, Bauer and Böhlke [24] investigated the linear closure, the orthotropic fitted closure [25], and the invariant-based optimal fitting closure [26]. In addition, the division of closure approximations into three groups was addressed: closures with algebraic assumptions as a background, closures based on material symmetry assumptions, and closures with an assumed orientation distribution function. Recently Tucker [27] proposed a new family of non-orthotropic closures for the special case of planar fiber orientation states to overcome the orthotropic limitation of closures depending on the intrinsically orthotropic second-order fiber orientation tensor as discussed by Bauer and Böhlke [28].

1.2. Originality

Accurate and consistent closure methods estimating the fourth-order orientation tensor needed for continuum mechanical computations are non-trivial to develop, since many algebraic properties have to be fulfilled: full index symmetry, trace condition, contraction condition, and the trace-preserving property of fiber orientation evolution equations. Furthermore, it is important to avoid computational effort in order to achieve attractive applications in numerical simulations. In view of this, the present manuscript contributes to the field of closure approximations with the following details:

- An implicit closure approach based on the contraction condition of fiber orientation tensors is proposed.
- Since the novel approach is formulated in a fully symmetric way, all necessary algebraic properties are fulfilled.
- Both the quadratic and the implicit formulation of the novel closure approach can be reduced to a one-dimensional nonlinear equation, whose unique solution is simple to determine.
- Besides both the quadratic and hybrid formulation of the novel closure method, any fully symmetric implicit extensions are possible within the proposed closure approach.
- It is shown that both considered fully symmetric implicit closures share the property of induced oscillations in simple shear flow. This behavior is no coincidence, as both implicit closures may be rigorously shown to approximate the maximum entropy closure.

1.3. Notation

Throughout this manuscript, scalars are denoted by, e.g., a, b and vectors by, e.g., \mathbf{a}, \mathbf{b} . Tensors of second order are represented by, e.g., \mathbf{A}, \mathbf{B} and fourth-order tensors refer to, e.g., \mathbb{A}, \mathbb{B} . The scalar product between tensors of equal order is denoted by, e.g., $\mathbf{A} \cdot \mathbf{B}$ with the Cartesian index representation $A_{ij}B_{ij}$. Please note that the scalar product, also known as complete contraction, is often denoted by, e.g., $\mathbf{A} \cdot \cdot \mathbf{B}$ or $\mathbf{A} : \mathbf{B}$ alternatively. The dyadic product is represented by, e.g., $\mathbf{A} \otimes \mathbf{B}$ with the Cartesian index representation $(\mathbf{A} \otimes \mathbf{B})_{ijkl} = A_{ij}B_{kl}$. The dyadic product between the same tensors is abbreviated by, e.g., $\mathbf{n} \otimes \mathbf{n} = \mathbf{n}^{\otimes 2}$.

By, e.g., $\mathbf{A} \square \mathbf{B}$ the box product is denoted with $(\mathbf{A} \square \mathbf{B})_{ijkl} = A_{ik}B_{lj}$ as the corresponding index notation. Mappings of equal-order tensors are given by, e.g., $\mathbf{A} \mathbf{B}$ reading $(\mathbf{A} \mathbf{B})_{ij} = A_{ik}B_{kj}$ in index notation. A mapping of a second-order tensor over a fourth-order tensor is denoted by, e.g., $\mathbb{A}[\mathbf{B}]$ with $(\mathbb{A}[\mathbf{B}])_{ij} = A_{ijkl}B_{kl}$ as the Cartesian index representation. The second-order identity tensor is represented by \mathbf{I} and $\mathbb{P}_1 = \mathbf{I} \otimes \mathbf{I} / 3$ refers to the identity on spherical second-order tensors. In contrast, $\mathbb{P}_2 = \mathbb{I}^S - \mathbb{P}_1$ refers to the identity on symmetric traceless second-order tensors with $\mathbb{I}^S = (\mathbf{I} \square \mathbf{I} + (\mathbf{I} \square \mathbf{I})^{\text{Tr}}) / 2$ representing the identity on symmetric second-order tensors. The operation $(\cdot)^{\text{Tr}}$ refers to a transposition of the right index pair of fourth-order tensors. The Frobenius tensor norm is denoted by $\|\cdot\|$ and $\text{tr}(\cdot)$ refers to the trace of a tensor.

2. The implicit closure approach

The present study considers the second- and fourth-order fiber orientation tensors of the first kind [1,2] defined as follows

$$\mathbf{N} = \int_S f(\mathbf{n}) \mathbf{n} \otimes \mathbf{n} \, dS, \quad \mathbb{N} = \int_S f(\mathbf{n}) \mathbf{n} \otimes \mathbf{n} \otimes \mathbf{n} \otimes \mathbf{n} \, dS, \quad (1)$$

with the non-polar orientation distribution function f , a probability density function which satisfies the symmetry condition $f(\mathbf{n}) = f(-\mathbf{n})$, where \mathbf{n} represents an arbitrary direction on the unit sphere S . The tensors given in Eq. (1) are totally symmetric, positive semi-definite and their trace is equal to one: $\text{tr}(\mathbf{N}) = \mathbf{N} \cdot \mathbf{I} = 1$ and $\text{tr}(\mathbb{N}) = \mathbb{N} \cdot (\mathbf{I} \square \mathbf{I}) = 1$. Closure approximations seek to approximate the fourth-order fiber orientation tensor \mathbb{N} as a function \mathbb{F} of the second-order fiber orientation tensor \mathbf{N}

$$\mathbb{N} \approx \mathbb{F}(\mathbf{N}). \quad (2)$$

Due to the relation $\mathbb{N}[\mathbf{I}] = \mathbf{N}$ [2] the second-order fiber-orientation tensor may be extracted from the fourth-order fiber orientation tensor. The inverse operation is not well-posed. In particular, there are different second-order fiber-orientation tensors realizing one and the same fourth-order fiber orientation tensor. It is noted that a closure is realizable if the value $\mathbb{F}(\mathbf{N})$ arises as the fourth moment of an orientation-distribution function. Different orientation distribution functions may lead to identical \mathbf{N} and \mathbb{N} , also with distinct sixth-order orientation $\mathbb{N}_{(6)}$. The novel implicit closure approach consists of using the property $\mathbb{N}[\mathbf{I}] = \mathbf{N}$ in terms of an arbitrary fully symmetric closure function \mathbb{F} with an unknown positive semi-definite and symmetric tensor \mathbf{B} instead of \mathbf{N} as the argument such that the contraction condition

$$\mathbb{F}(\mathbf{B})[\mathbf{I}] = \mathbf{N} \quad (3)$$

is satisfied. Eq. (3) implies that \mathbf{B} is a function of \mathbf{N} for a chosen closure function.¹ In order to approximate the fourth-order orientation tensor \mathbb{N} in terms of $\mathbb{F}(\mathbf{B})$ the equation

$$\mathbf{F}(\mathbf{B}) = \mathbf{0} \quad (4)$$

has to be solved for the tensor \mathbf{B} with the function $\mathbf{F}(\mathbf{B})$ defined as follows

$$\mathbf{F}(\mathbf{B}) = \mathbb{F}(\mathbf{B})[\mathbf{I}] - \mathbf{N}. \quad (5)$$

In general, $\mathbf{F}(\mathbf{B})$ is non-linear in \mathbf{B} which is why Newton's method is used as follows

$$\mathbf{B}_{n+1} = \mathbf{B}_n - \left(\frac{\partial \mathbf{F}(\mathbf{B}_n)}{\partial \mathbf{B}_n} \right)^{-1} [\mathbf{F}(\mathbf{B}_n)] \quad (6)$$

with an appropriate initial guess, e.g., $\mathbf{B}_0 = \mathbf{N}$ and n as the iteration index. The previously described relationship between the orientation

¹ Formally, the approximation $\mathbb{N} \approx \mathbb{F}(\mathbf{N})$ is replaced by $\mathbb{N} \approx \mathbb{G}(\mathbf{B})$. In general, the tensors \mathbf{B} and \mathbf{N} are connected via $\mathbf{H}(\mathbf{B}) = \mathbf{N}$ leading to the alternative formulation of the closure approximation $\mathbb{F}(\mathbf{N}) = \mathbb{G}(\mathbf{H}^{-1}(\mathbf{N}))$.

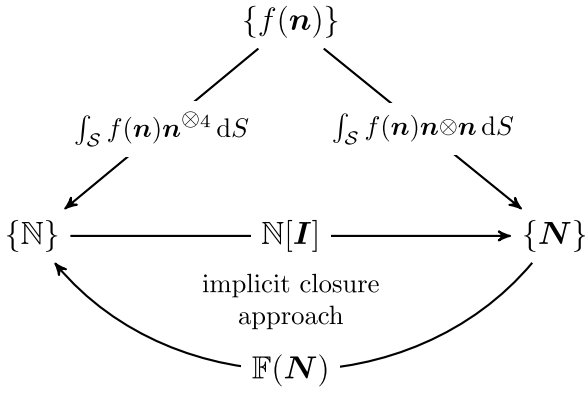


Fig. 1. Graphical representation of the relationship between the orientation distribution function f and the fiber orientation tensors N and \mathbb{N} for a realizable closure function $\mathbb{F}(N)$.

distribution function f and the fiber orientation tensors N and \mathbb{N} is shown graphically for a realizable closure function $\mathbb{F}(N)$ in Fig. 1. In particular, it is illustrated that the implicit closure approach is located between the fiber orientation tensors N and \mathbb{N} based on the contraction property $\mathbb{N}[I] = N$.

A fully symmetric closure that fulfills $\mathbb{N}[I] = N$ implies the trace condition of the fourth-order orientation tensor $\text{tr}(\mathbb{N}) = 1$ (see, e.g., Karl et al. [12]). In addition, the consistency with the flow $\text{tr}(\mathbb{N}[D]) = N \cdot D$ in the context of the Folgar–Tucker equation [2,11,16] is also fulfilled by imposing $\mathbb{N}[I] = N$ in view of the fully symmetric implicit approach with D representing the symmetric part of the velocity gradient

$$\text{tr}(\mathbb{N}[D]) = N_{ikl} D_{kl} = \mathbb{N}[I] \cdot D = N \cdot D. \quad (7)$$

It should be noted that N is seen as the exact second-order orientation tensor fulfilling all necessary algebraic properties, e.g., the trace condition, the symmetry condition and positive semi-definiteness.

3. The fully symmetric implicit quadratic closure

3.1. Definition

The closure function for the symmetric implicit quadratic closure (SIQ) reads as follows

$$\mathbb{F}(B) = \text{sym}(B \otimes B) = \frac{1}{3} (B \otimes B + B \square B + (B \square B)^T). \quad (8)$$

By inserting Eq. (8) in Eq. (5) the function $F(B)$ is derived for the SIQ closure as follows given both in symbolic and in index notation

$$F(B) = \frac{1}{3} (\text{tr}(B)B + 2B^2) - N, \quad (9)$$

$$F_{ij}(B) = \frac{1}{3} (B_{kk}B_{ij} + 2B_{ik}B_{kj}) - N_{ij}.$$

3.2. Solution procedure

In this section it is shown that Eq. (4) with $F(B)$ given in Eq. (9) admits a symmetric positive semi-definite solution B for any given symmetric positive semi-definite orientation tensor N . A constructive approach is used which turns out to be useful for numerical computations. This approach also shows that the solution is in fact unique.

By using the abbreviation $s = \text{tr}(B)/4$ the defining Eq. (9) can be written in the form

$$B^2 + 2sB = \frac{3}{2}N, \quad (10)$$

which can be reformulated by completing the square as follows

$$(B + sI)^2 = \frac{3}{2}N + s^2I. \quad (11)$$

Since N is positive semi-definite, as addressed above, the following representation of the sought tensor B can be obtained

$$B = \sqrt{\frac{3}{2}N + s^2I} - sI. \quad (12)$$

It should be noted that for computing B based on Eq. (12), only the scalar variable s has to be determined. In order to derive an equation for s , the trace of both sides of Eq. (12) is taken, yielding

$$4s = \text{tr} \left(\sqrt{\frac{3}{2}N + s^2I} \right) - d s, \quad (13)$$

with $d = 2, 3$ representing the dimension of the considered problem. To proceed, it is noted that the tensors N and B share the same eigensystem. That N and B commute and are thus jointly diagonalizable is shown by multiplying Eq. (9) on the left and on the right by the tensor B leading to

$$NB = \frac{1}{3} (\text{tr}(B)B^2 + 2B^3) = BN. \quad (14)$$

With λ_i representing the given eigenvalues of N , the defining equation (13) for s becomes

$$(d + 4)s = \sum_{i=1}^d \sqrt{\frac{3\lambda_i}{2} + s^2}. \quad (15)$$

Once Eq. (15) is solved for s , the eigenvalues μ_i of B can be computed based on the following equation representing Eq. (12) in the eigensystem of B

$$\mu_i = \sqrt{\frac{3\lambda_i}{2} + s^2} - s. \quad (16)$$

The eigenvalues μ_i refer to the diagonal matrix \tilde{B}_{ij} as the eigensystem representation of B_{ij} with $B_{ij} = Q_{ik} \tilde{B}_{kl} Q_{lj}^T$ being the eigendecomposition of B_{ij} with an orthogonal matrix $Q_{ij} \in \text{Orth}^+$.

For any $\lambda_i \geq 0$, Eq. (15) is uniquely solvable. Indeed, the following continuous function is considered

$$f : \mathbb{R}_{\geq 0} \rightarrow \mathbb{R}, \quad s \mapsto (d + 4)s - \sum_{i=1}^d \sqrt{\frac{3\lambda_i}{2} + s^2}, \quad (17)$$

whose roots s correspond to solutions of Eq. (16). Estimating the derivative of the function f from below

$$f'(s) = d + 4 - \sum_{i=1}^d \frac{s}{\sqrt{\frac{3\lambda_i}{2} + s^2}} = 4 + \sum_{i=1}^d \underbrace{\left(1 - \frac{s}{\sqrt{\frac{3\lambda_i}{2} + s^2}} \right)}_{\geq 0} \geq 4, \quad (18)$$

it is observed that the function f is strongly monotone. Indeed, due to $\lambda_i \geq 0$ the following inequality holds

$$\sqrt{\frac{3\lambda_i}{2} + s^2} \geq s \quad \text{implies} \quad 1 \geq \frac{s}{\sqrt{\frac{3\lambda_i}{2} + s^2}}. \quad (19)$$

Thus, any root of the function f is unique. To show the existence of a root, it is observed that

$$f(0) = - \sum_{i=1}^d \sqrt{\frac{3\lambda_i}{2}} \leq 0. \quad (20)$$

Furthermore, the estimate (18) implies

$$f(s) = f(0) + \int_0^s f'(\tau) d\tau \geq f(0) + 4s \rightarrow \infty \quad (21)$$

as $s \rightarrow \infty$. In particular f attains the value 0 and Eq. (15) is solvable. Concerning the uniqueness, notice that B is determined, by the mean-value theorem, solely from computed s and given N , see Eq. (12). Moreover, Eq. (15) for s is uniquely solvable. Thus, there is only one solution B to Eq. (9).

3.3. Realizability by a fiber-orientation distribution

In two and three spatial dimensions ($d = 2, 3$), each completely symmetric fourth-order tensor \mathbb{N} can be written in the form

$$\mathbb{N} = \sum_{i=1}^l \kappa_i \mathbf{r}_i^{\otimes 4} \quad (22)$$

for a non-negative integer l , non-negative numbers κ_i and vectors $\mathbf{r}_i \in \mathbb{R}^d$ ($i = 1, \dots, l$) if and only if the tensor \mathbb{N} is completely symmetric and positive semi-definite in the sense

$$\mathbf{S} \cdot \mathbb{N}[\mathbf{S}] \geq 0 \quad \forall \quad \mathbf{S} = \mathbf{S}^T, \quad (23)$$

see Bauer et al. [29]. Thus, the SIQ closure given in Eq. (8) is realized by a fiber-orientation distribution precisely if the following condition holds for all symmetric second-order tensors \mathbf{S}

$$\mathbf{S} \cdot \text{sym}(\mathbf{B} \otimes \mathbf{B})[\mathbf{S}] \geq 0. \quad (24)$$

Next it is shown that this condition holds provided that \mathbf{B} is positive semi-definite. Using Eq. (8) in index notation one can write

$$\begin{aligned} 3\mathbf{S} \cdot \text{sym}(\mathbf{B} \otimes \mathbf{B})[\mathbf{S}] &= S_{ij} B_{ij} B_{kl} S_{kl} + S_{ij} B_{ik} B_{lj} S_{kl} + S_{ij} B_{il} B_{kj} S_{kl} \\ &= S_{ij} B_{ij} S_{kl} B_{kl} + 2S_{ij} B_{jl} S_{ik} B_{ki} \\ &= (\mathbf{S} \cdot \mathbf{B})^2 + 2\text{tr}(\mathbf{S} \mathbf{B} \mathbf{S} \mathbf{B}). \end{aligned} \quad (25)$$

Both summands are non-negative. For the first summand, this is trivial. The assertion for the second summand follows from the fact that the following inequality holds for symmetric and positive semi-definite \mathbf{B} and \mathbf{C}

$$\mathbf{B} \cdot \mathbf{C} \geq 0. \quad (26)$$

Indeed, an eigendecomposition of the tensor \mathbf{B} shows the inequality (26)

$$\mathbf{B} = \sum_{i=1}^d \mu_i \mathbf{r}_i \otimes \mathbf{r}_i, \quad \mathbf{B} \cdot \mathbf{C} = \sum_{i=1}^d \underbrace{\mu_i}_{\geq 0} \underbrace{\mathbf{C} \cdot (\mathbf{r}_i \otimes \mathbf{r}_i)}_{\geq 0} \geq 0. \quad (27)$$

Applying this result to \mathbf{B} and the symmetric and non-negative tensor $\mathbf{C} = \mathbf{S} \mathbf{B} \mathbf{S}$ gives the following result that the condition (24) holds

$$\text{tr}(\mathbf{S} \mathbf{B} \mathbf{S} \mathbf{B}) = \mathbf{B} \cdot (\mathbf{S} \mathbf{B} \mathbf{S}) = \mathbf{B} \cdot \mathbf{C} \geq 0 \quad (28)$$

and the SIQ closure is realizable. With a similar line of reasoning it can be shown that the symmetric quadratic closure [12] is also realizable with \mathbf{N} instead of \mathbf{B} in view of the calculations outlined above.

3.4. Exactness for UD, ISO and PI orientation states

In this section it is considered whether the unidirectional (UD), isotropic (ISO) and planar isotropic (PI) orientation states are exactly realized by the SIQ closure approach. For simplicity, it suffices to consider \mathbf{N} and \mathbf{B} in an eigensystem representation. Furthermore, is noted that $\mu_i = 0$ is a direct consequence of $\lambda_i = 0$ via the chain of equalities

$$\mu_i = \sqrt{\frac{3\lambda_i}{2} + s^2} - s = \sqrt{s^2} - s = 0. \quad (29)$$

In addition, the latter equation also shows that if multiple eigenvalues $\lambda_i = \lambda_j$ are given, the relation $\mu_i = \mu_j$ will follow directly.

First, the UD case is considered with $\lambda_1 = 1$ and $\lambda_2 = \lambda_3 = 0$. As a consequence, $\mu_2 = \mu_3 = 0$ holds and the equation for μ_1 reduces to $\mu_1^2 = 1 \leftrightarrow \mu_1 = 1$ by inserting $s = \mu_1/4$. Therefore, the SIQ closure $\mathbb{N}(\mathbf{B}) = \text{sym}(\mathbf{B} \otimes \mathbf{B})$ results in the exact tensor for the UD case $\mathbb{N}_{\text{UD}} = \mathbf{e}_1^{\otimes 4}$ [12,30].

Second, the ISO case is considered with $\lambda_1 = \lambda_2 = \lambda_3 = \lambda = 1/3$ and, therefore, with the form $\mathbf{B} = \mu \mathbf{I}$ based on $\mu_1 = \mu_2 = \mu_3 = \mu$. The governing equation (9) for the SIQ closure implies

$$\frac{1}{3} \mathbf{I} = \frac{1}{3} (3\mu^2 \mathbf{I} + 2\mu^2 \mathbf{I}) \quad \leftrightarrow \quad \frac{1}{3} = \mu^2 + \frac{2}{3} \mu^2, \quad (30)$$

leading to $1 = 5\mu^2$ with the physically consistent solution $\mu = 1/\sqrt{5}$, or $\mathbf{B} = \mathbf{I}/\sqrt{5}$, respectively. In a next step, this result is inserted into Eq. (8), leading to

$$\text{sym}(\mathbf{B} \otimes \mathbf{B}) = \frac{1}{15} (\mathbf{I} \otimes \mathbf{I} + \mathbf{I} \square \mathbf{I} + (\mathbf{I} \square \mathbf{I})^T) = \frac{1}{3} \mathbb{P}_1 + \frac{2}{15} \mathbb{P}_2 = \mathbb{N}_{\text{ISO}}, \quad (31)$$

representing the exact expression for the isotropic fourth-order orientation tensor [12,30].

Third, the PI case is considered with $\lambda_1 = \lambda_2 = \lambda = 1/2$ and $\lambda_3 = 0$. Therefore, the relations $\mu_1 = \mu_2 = \mu$ and $\mu_3 = 0$ hold. By using the governing equation (9) for the SIQ closure, one deduces with the two-dimensional identity tensor $\mathbf{I}_{(2)}$

$$\frac{1}{2} \mathbf{I}_{(2)} = \frac{1}{3} (2\mu^2 \mathbf{I}_{(2)} + 2\mu^2 \mathbf{I}_{(2)}) \quad \leftrightarrow \quad \frac{1}{2} = \frac{4}{3} \mu^2, \quad (32)$$

leading to the physically consistent solution $\mu = \sqrt{3/8}$ or $\mathbf{B} = \sqrt{3/8} \mathbf{I}$, respectively. Proceeding as for the previous cases, inserting this result into Eq. (8) leads to

$$\text{sym}(\mathbf{B} \otimes \mathbf{B}) = \frac{1}{8} (\mathbf{I}_{(2)} \otimes \mathbf{I}_{(2)} + \mathbf{I}_{(2)} \square \mathbf{I}_{(2)} + (\mathbf{I}_{(2)} \square \mathbf{I}_{(2)})^T), \quad (33)$$

or equivalently

$$\text{sym}(\mathbf{B} \otimes \mathbf{B})_{ijkl} = \frac{1}{8} (\delta_{ij} \delta_{kl} + \delta_{ik} \delta_{jl} + \delta_{il} \delta_{kj}), \quad (34)$$

$i, j, k, l \in \{1, 2\}$, which corresponds to the exact expression for the planar isotropic fourth-order orientation tensor [12,30].

4. The fully symmetric implicit hybrid closure

4.1. Definition and solution procedure

The second proposed closure combines the SIQ closure discussed in the previous Section 3 with the well-known hybrid approach [2,8]. This closure is named fully symmetric implicit hybrid closure (SIHYB) and fixes the lack of symmetry of the original hybrid closure addressed by, e.g., Petty et al. [11]. The respective closure function reads

$$\mathbb{F}(\mathbf{B}) = (1 - k) \left(-\frac{3}{35} \text{sym}(\mathbf{I} \otimes \mathbf{I}) + \frac{6}{7} \text{sym}(\mathbf{I} \otimes \mathbf{B}) \right) + k \text{sym}(\mathbf{B} \otimes \mathbf{B}), \quad (35)$$

with $k = 1 - 27 \det(\mathbf{N})$ for three-dimensional fiber orientation states. The two-dimensional case proceeds similarly by adapting the definition of k and the prefactors of the linear part in Eq. (35) as given in, e.g., Advani and Tucker [8]. Analogous to the SIQ closure, the function $\mathbb{F}(\mathbf{B})$ defined in Eq. (5) is formulated as follows given both in symbolic and in index notation for the SIHYB closure in order to compute the tensor \mathbf{B} based on Eq. (4)

$$\begin{aligned} \mathbf{F}(\mathbf{B}) &= \frac{1-k}{7} (\text{tr}(\mathbf{B}) - 1) \mathbf{I} + \left(1 - k + \frac{k}{3} \text{tr}(\mathbf{B}) \right) \mathbf{B} + \frac{2k}{3} \mathbf{B}^2 - \mathbf{N}, \\ \mathbb{F}_{ij}(\mathbf{B}) &= \frac{1-k}{7} (B_{mn} - 1) \delta_{ij} + \left(1 - k + \frac{k}{3} B_{mn} \right) B_{ij} + \frac{2k}{3} B_{in} B_{nj} - N_{ij}. \end{aligned} \quad (36)$$

Similar to SIQ, SIHYB can be reduced to a one-dimensional formulation as shown in Appendix A. It should be noted that the symmetric hybrid closure proposed by Petty et al. [11] differs in the quadratic term and, in particular, no implicit formulation was addressed.

4.2. Exactness for UD, ISO and PI orientation states

For the UD case, $k = 1$ holds and the SIHYB closure corresponds to the SIQ closure, for which the exactness for UD is shown in Section 3.4. For the ISO case, $k = 0$ follows, leading to the linear equation for \mathbf{B}

$$\frac{1}{7} (\text{tr}(\mathbf{B}) - 1) \mathbf{I} + \mathbf{B} - \frac{1}{3} \mathbf{I} = \mathbf{0}. \quad (37)$$

As a consequence, \mathbf{B} is also isotropic with $\mathbf{B} = \mu \mathbf{I}$ leading to $\mu = 1/3$. By inserting the latter result into the linear part of Eq. (35), the isotropic fourth-order orientation tensor is obtained. Within a three-dimensional description, a PI orientation state leads to $k = 1$ with SIHYB corresponding to SIQ. As already addressed in Section 3.4, the SIQ closure is exact for PI.

4.3. Remarks on the realizability by a fiber-orientation distribution

Since the realizability by a fiber-orientation distribution is shown above for the SIQ closure, the linear closure as the second part of the SIHYB closure is discussed in the section at hand. As pointed out by Bauer and Böhlke [24], the linear closure approximation represents a purely algebraic assumption. In addition, the corresponding fourth-order orientation tensor of the third kind [1], representing a measure of anisotropy, is zero. It was also addressed by Bauer and Böhlke [24] that the linear closure may violate the allowed parameter space. As a consequence, orientation states exist for which the linear closure predicts non-realizable fourth-order orientation tensors. Since the hybrid closure approach is based on a linear interpolation between the linear and the quadratic closure, the realizability by a fiber-orientation distribution is not ensured, in general. Nevertheless, the SIHYB closure approach is used in the following Section 5 together with the SIQ closure in order to investigate the applicability in view of orientation evolution and prediction of anisotropic viscous and elastic properties.

5. Numerical examples

5.1. Prediction of fiber orientation evolution

In the present section, the proposed SIQ and SIHYB closures are investigated with respect to the predicted orientation evolution. For clarity, only a simple shear flow is considered, with the strain rate tensor \mathbf{D} and the spin tensor \mathbf{W} prescribed as follows

$$\begin{aligned}\mathbf{D} &= \dot{\gamma}(e_1 \otimes e_2 + e_2 \otimes e_1)/2, \\ \mathbf{W} &= \dot{\gamma}(e_1 \otimes e_2 - e_2 \otimes e_1)/2.\end{aligned}\quad (38)$$

The tensor \mathbf{D} is the symmetric part of the velocity gradient $\mathbf{L} = \dot{\gamma} e_1 \otimes e_2$ and \mathbf{W} is the skew-symmetric part of \mathbf{L} , respectively. The shear rate $\dot{\gamma}$ can be chosen arbitrarily since the results are considered in view of the total shear $\dot{\gamma}t$, $t_0 = 0$. The orientation evolution is governed by the Folgar–Tucker equation [2,16]

$$\dot{\mathbf{N}} = \mathbf{W}\mathbf{N} - \mathbf{N}\mathbf{W} + \xi(\mathbf{D}\mathbf{N} + \mathbf{N}\mathbf{D} - 2\mathbb{F}[\mathbf{D}]) + 2C_1\dot{\gamma}(\mathbf{I} - 3\mathbf{N}). \quad (39)$$

In Eq. (39), the shape parameter ξ depends on the fiber aspect ratio α via $\xi = (\alpha^2 - 1)/(\alpha^2 + 1)$. The intensity of fiber–fiber interaction is represented by the fiber interaction parameter C_1 (also called interaction coefficient or Folgar–Tucker diffusivity) and $\dot{\gamma} = \sqrt{2\mathbf{D} \cdot \mathbf{D}}$ refers to the equivalent shear rate. Depending on the closure approach in use, the closure function \mathbb{F} refers to $\mathbb{F}(\mathbf{B})$ in terms of the proposed implicit closures SIQ and SIHYB. Regarding the classical closures, the closure function \mathbb{F} refers to $\mathbb{F}(\mathbf{N})$. Within the present study, the following closures and fiber orientation distribution estimations are considered in order to compare the results with the SIQ and SIHYB closures:

- Quadratic closure (QC) [2,8,9]

$$\mathbb{F}(\mathbf{N}) = \mathbf{N} \otimes \mathbf{N} \quad (40)$$

- Symmetric quadratic closure (SQC) for fiber orientation evolution description [12]

$$2\mathbb{F}(\mathbf{N}) = \kappa \operatorname{sym}(\mathbf{N} \otimes \mathbf{N}) \quad (41)$$

with

$$\kappa = \begin{cases} 0, & \mathbf{N} = \mathbf{N}_{\text{ISO}}, \mathbf{D} = \mathbf{0} \\ \frac{6\mathbf{N} \cdot \mathbf{D}}{\mathbf{N} \cdot \mathbf{D} + 2\mathbf{D} \cdot \mathbf{N}^2}, & \mathbf{N} \neq \mathbf{N}_{\text{ISO}}, \mathbf{D} \neq \mathbf{0} \end{cases} \quad (42)$$

- Hybrid closure (HYB) [2,8]

$$\begin{aligned}\mathbb{F}(\mathbf{N}) &= (1 - k) \left(-\frac{3}{35} \operatorname{sym}(\mathbf{I} \otimes \mathbf{I}) + \frac{6}{7} \operatorname{sym}(\mathbf{I} \otimes \mathbf{N}) \right) + k \mathbf{N} \otimes \mathbf{N}, \\ k &= 1 - 27 \det(\mathbf{N})\end{aligned}\quad (43)$$

- Invariant-based optimal fitting closure (IBOF) with β_i depending on the invariants of \mathbf{N} [26]

$$\begin{aligned}\mathbb{F}(\mathbf{N}) &= \beta_1 \operatorname{sym}(\mathbf{I} \otimes \mathbf{I}) + \beta_2 \operatorname{sym}(\mathbf{I} \otimes \mathbf{N}) \\ &+ \beta_3 \operatorname{sym}(\mathbf{N} \otimes \mathbf{N}) + \beta_4 \operatorname{sym}(\mathbf{I} \otimes \mathbf{N}^2) \\ &+ \beta_5 \operatorname{sym}(\mathbf{N} \otimes \mathbf{N}^2) + \beta_6 \operatorname{sym}(\mathbf{N}^2 \otimes \mathbf{N}^2)\end{aligned}\quad (44)$$

- Maximum entropy closure (MEM) based on the Bingham distribution [31–35]²

$$f(\mathbf{n})_{\text{MEM}} = c \exp(\tilde{\mathbf{G}} \cdot \mathbf{n} \otimes \mathbf{n}) = \exp(\mathbf{G} \cdot \mathbf{n} \otimes \mathbf{n}) \quad (45)$$

- Fast exact closure based on the angular central Gaussian distribution (ACG) [13–15] also known as the natural closure of Verleye and Dupret [37]

$$f(\mathbf{n})_{\text{ACG}} = \frac{1}{4\pi} (\mathbf{G} \cdot \mathbf{n} \otimes \mathbf{n})^{-\frac{3}{2}} \quad (46)$$

As pointed out by Mehta and Schneider [38] the tensor \mathbf{G} has to be computed for both the MEM and ACG closure based on

$$\mathbf{0} = \mathbf{N} - \int_S f(\mathbf{n}) \mathbf{n} \otimes \mathbf{n} \, dS, \quad (47)$$

with $f(\mathbf{n})$ representing either Eq. (45) or (46). For details about the ACG solution procedure, the reader is referred to Mehta and Schneider [38] and for the MEM solution procedure, further details can be found in Müller and Böhlke [35]. Within this study, the numerical integration scheme of Lebedev and Laikov [39] is used with the implementation of Parrish [40] for evaluating the integrals over the unit sphere S in order to determine \mathbf{G} and the sought tensor \mathbf{N} . The maximum number of 5810 integration points on S is used, and the tolerance for ACG and MEM is set to 10^{-8} . The initial guess $s_0 = 0.25$ is fixed for both SIQ and SIHYB.

In Fig. 2, the evolution of the orientation component N_{11} is shown for the fiber interaction parameters $C_1 = 0$ and $C_1 = 0.005$ in response to the total shear $\dot{\gamma}t$. In addition, the shape parameter $\xi = 1$ ($\alpha \rightarrow \infty$) is fixed. The Folgar–Tucker equation (39) is integrated with a fourth-order Runge–Kutta method [41] and a time step size of $\Delta t = 0.01$ s. As a reference solution without closure-induced errors the numerical solution of the Fokker–Planck equation [42] for the orientation distribution function $f(t, \mathbf{x}, \mathbf{n})$ additionally depending on the spatial position \mathbf{x} and the time t extended by the isotropic diffusion term on the unit sphere S [15,43]

$$\dot{f} + \operatorname{div}_S(f\dot{\mathbf{n}}) = C_1 \dot{\gamma} \Delta_S(f) \quad (48)$$

is also shown in Fig. 2. In Eq. (48) $\dot{\gamma}$ and C_1 refer to the definitions in the context of the Folgar–Tucker equation (39), \dot{f} represents the materials time derivative with respect to t and \mathbf{x} . The divergence and the Laplacian on the unit sphere are denoted by $\operatorname{div}_S(\cdot)$ and $\Delta_S(\cdot)$. Tucker's implementation [44] is used for the numerical solution of Eq. (48) with 150×150 grid points on the unit hemisphere and a maximum Courant number of 0.1. The well-known periodic orientation behavior [14,45], which is also called Jeffery orbits [46–48] is not present for $C_1 = 0$ in the left part of Fig. 2 since the period length $T = 2\pi/(\dot{\gamma}\sqrt{1 - \xi^2})$ [14,46] is infinitely large for $\xi = 1$. On the other hand, a non-zero fiber interaction parameter $C_1 = 0.005$ reduces the high alignment level of a vanishing fiber interaction parameter $C_1 = 0$ due to the present diffusive effect towards the isotropic state. The behavior of the common closures is well studied in the literature and, therefore, not focused in the present study: QC and HYB [2,8], SQC [12], IBOF [26,49,50] and ACG [14]. In summary, QC and HYB overestimate the alignment of the fibers and SQC is a useful ad-hoc improvement of QC. In particular, the ACG closure is exact for the

² In the recent publication of Papenfuss [36] an explicit MEM-based estimation of $f(\mathbf{n})$ is proposed using a function regarding the underlying information-theoretic entropy.

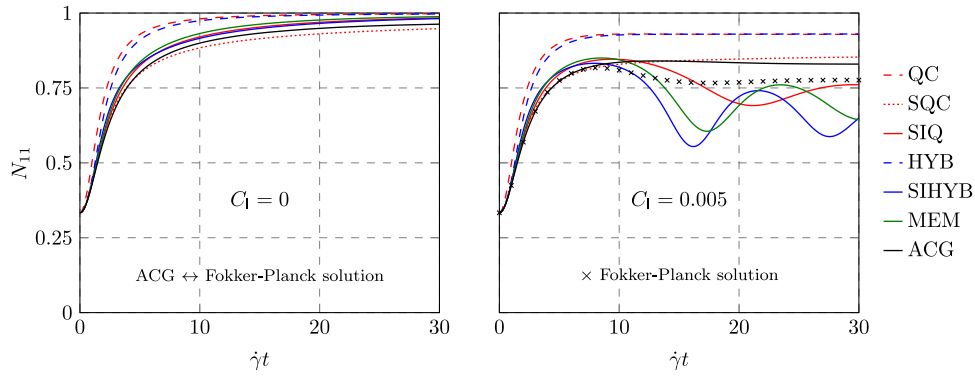


Fig. 2. Evolution of the orientation tensor component N_{11} plotted over the total shear $\dot{\gamma}t$ for two different values of fiber interaction parameter C_1 with respect to different closure approximations in a simple shear flow given in Eq. (38).

case of absent fiber–fiber interaction [14,15,37] (and, therefore, represents the solution of the Fokker–Planck equation for a vanishing fiber interaction parameter $C_1 = 0$) and the IBOF closure approximates the ACG-related orientation results closely. Therefore, the IBOF results are not shown in Fig. 2. It should be noted that the overshoot of IBOF and ACG with respect to the Fokker–Planck solution is well known [26,50]. Regarding the proposed implicit closures and the MEM-related results, a distinct oscillatory orientation behavior is observed for $C_1 = 0.005$ compared to all other shown closures. The oscillations increase in the order SIQ→MEM→SIHYB. In particular, IBOF and ACG also show a weak oscillatory orientation behavior with one single peak at $\dot{\gamma}t \approx 10$. In contrast, vanishing fiber interaction parameter $C_1 = 0$ leads to a stable solution behavior as shown in the left plot in Fig. 2. This suggests that for SIQ, SIHYB, and MEM the fiber interaction parameter C_1 has a destabilizing effect and induces the oscillations due to the interaction between the closure term and the diffusion term within the Folgar–Tucker equation. Surprisingly, the proposed implicit closures show very good agreement with the MEM approach. In conclusions, SIQ and SIHYB are capable of replacing the MEM with regard to a low-cost computation. In this context, SIHYB is more accurate than SIQ in view of approximating the MEM results with respect to orientation evolution.

To further investigate the oscillatory behavior, the ACG, MEM and both new closures SIQ and SIHYB are compared against each other for various interaction parameters C_1 . In addition, the solution of the Fokker–Planck equation is used as the reference in Fig. 3 showing the orientation evolution of the tensor component N_{11} with respect to the total shear $\dot{\gamma}t$. The results show that both proposed implicit closures behave similar to MEM over the considered range of the fiber interaction parameter C_1 . With decreasing values of the fiber interaction parameter C_1 the period length of the oscillation increases and for $C_1 = 5 \cdot 10^{-5}$ and $C_1 = 5 \cdot 10^{-6}$ oscillations induced by parameter values $C_1 > 0$ are not observed in the shown range of total shear. For SIQ, the amplitude of the oscillations halved at a total shear $\dot{\gamma}t \approx 1000$, while for SIHYB this occurs at a total shear $\dot{\gamma}t \approx 1700$. For high values of C_1 (higher than 0.05 which is typically not realized in physical situations) the oscillations are damped due to the strong diffusion towards the isotropic state. For typical values of C_1 in the interval $[5 \cdot 10^{-4}, 5 \cdot 10^{-3}]$ the oscillations for MEM, SIQ, and SIHYB are distinct in the shown range and lead to inadequate accuracy of the orientation tensor results compared to the Fokker–Planck solution. It should be noted that the fiber interaction parameter C_1 is typically selected accounting for the fiber aspect ratio and the fiber volume fraction [51,52]. Additional computational experiments regarding the widely used reduced-strain closure model (RSC) [53] and anisotropic rotary diffusion model (ARD) [54] show that the oscillations are still present with the oscillations of SIHYB being more distinct compared to SIQ.

As already addressed, the proposed SIQ and SIHYB closures behave like the MEM closure. This empirical observation may be backed up

by theoretical arguments. In general, the closure principle of the MEM is based on maximizing the information-theoretic entropy η which leads to an orientation distribution function that is as isotropic (or as uniform) as possible [27], but reproduces a given finite number of statistical moments. In the recent publication of Papenfuss [36] the series expansion

$$\eta = \eta_0 + \frac{1}{2}\eta_2\text{tr}(\mathbb{N}'^2) + \frac{1}{6}\eta_3\text{tr}(\mathbb{N}'^3) + \mathcal{O}(\mathbb{N}'^4) \quad (49)$$

of the information-theoretic entropy [27,31]

$$\eta = - \int_S f(\mathbf{n})\ln(f(\mathbf{n})) \, dS \quad (50)$$

is considered in terms of the symmetric and traceless (also known as irreducible) second-order fiber orientation tensor of the third kind \mathbb{N}' [1]. It should be noted that orientation tensors of the third kind represent measures of anisotropy. Therefore, the η_0 -term in Eq. (49) represents the isotropic part and all other terms of the power series (49) contain information about the microstructure’s anisotropy. Papenfuss [36] derived the following lowest order MEM approximation for the irreducible fourth-order orientation tensor \mathbb{N}' based on the series expansion (49)

$$\mathbb{N}' \approx \frac{4\eta_2^2}{315}(\mathbb{N}' \otimes \mathbb{N}')'. \quad (51)$$

Eq. (51) is reformulated as follows in terms of \mathbb{N} and \mathbb{N} using the relationships between the tensors \mathbb{N} and \mathbb{N}' and between the tensors \mathbb{N} and \mathbb{N}' [1,2]

$$\mathbb{N} \approx -\frac{3}{35}\text{sym}(\mathbb{I} \otimes \mathbb{I}) + \frac{6}{7}\text{sym}(\mathbb{I} \otimes \mathbb{N}) + \frac{4\eta_2^2}{315}\mathbb{A}_{(8)} \left[(\mathbb{N} - \mathbb{I}/3) \otimes (\mathbb{N} - \mathbb{I}/3) \right], \quad (52)$$

with $\mathbb{A}_{(8)}$ as the identity on irreducible fourth-order tensors. Eq. (52) states that the lowest order approximation of the MEM closure refers to a fully symmetric expressions of linear and quadratic order in the orientation tensor \mathbb{N} . Thus, the proposed implicit closures SIQ and SIHYB may be interpreted as lowest order MEM approximations accounting for the constraint $\mathbb{N}[\mathbb{I}] = \mathbb{N}$ which refers to the formulation $\mathbb{F}(\mathbb{N})[\mathbb{I}] = \mathbb{N}$ in terms of the closure function \mathbb{F} . The difference to the MEM lies in the implicit procedure represented by replacing the orientation tensor \mathbb{N} by the closure tensor \mathbb{B} within the closure function \mathbb{F} . It is noticed in the computational experiments that SIHYB is a better approximation of the MEM compared to SIQ. This is because SIHYB is closer to the lowest order approximation of MEM than SIQ due to the combination of linear and quadratic terms in the hybrid approach. Interestingly, the classical QC and HYB closures do not show oscillations. However, these closures do not have the required full index symmetry and, therefore, cannot be understood as a lowest order approximation of the MEM.

The recent publication of Tucker [27] also addresses non-physical oscillations of the MEM closure within a simple shear flow for typical

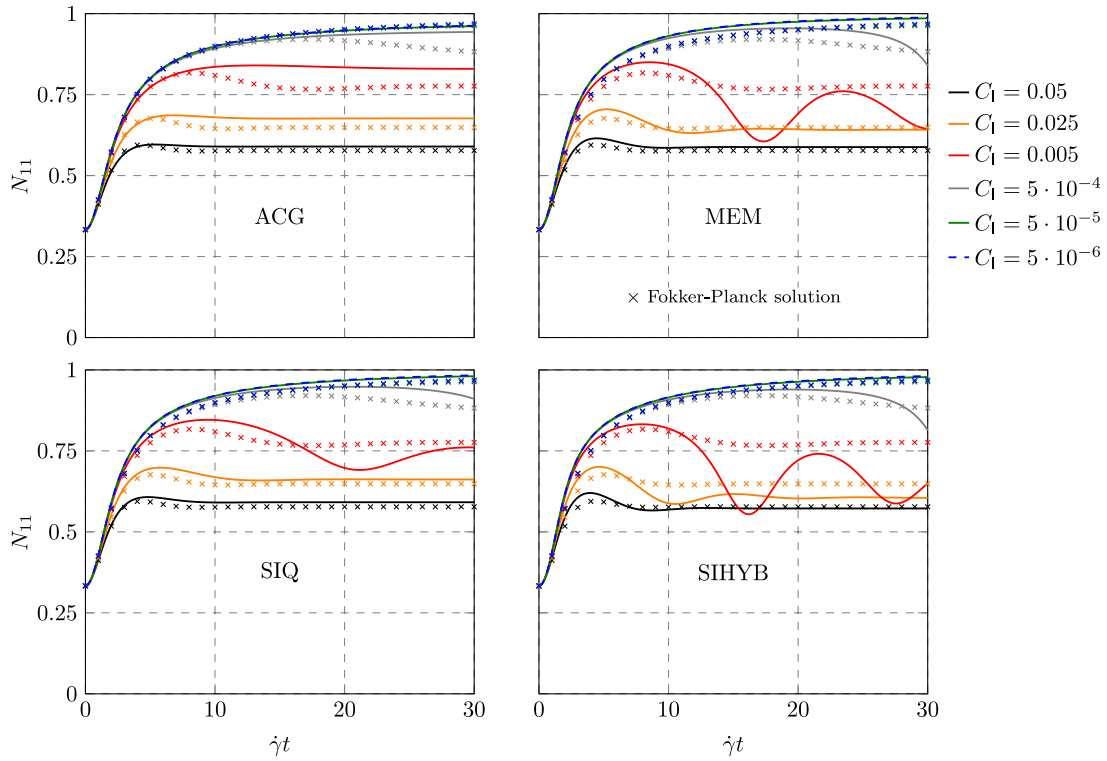


Fig. 3. Evolution of the orientation tensor component N_{11} plotted over the total shear $\dot{\gamma}t$ for different values of fiber interaction parameter C_1 with respect to ACG, MEM, SIQ and SIHYB in a simple shear flow given in Eq. (38).

fiber interaction parameter values C_1 . It is stated that the MEM closure (or the underlying Bingham distribution) is not an accurate approximation of orientation distributions which occur during flow processes. As SIQ and SIHYB may be considered as approximations of the MEM, it does not come as a surprise that these closures feature oscillations in shear flow, as well. It should be noted that the MEM closure is evaluated as accurate by Chaubal and Leal [33] and Feng et al. [55] with respect to non-approximated solutions for liquid-crystalline polymers. However, these studies are based on a different orientation evolution equation, which differs from the Folgar–Tucker equation by a nematic term.

To conclude this section, reference is made to Montgomery–Smith [56–58] addressing instabilities (growth of perturbations) of Jeffery’s equation in the context of flow-fiber coupling caused by fiber-induced anisotropic viscosity within the balance of linear momentum.

5.2. Prediction of anisotropic viscosity and stiffness

In the present section all considered closure approximations are compared in view of predicting the viscous and elastic anisotropy for the following measured orientation state³ [59]

$$N_{ij} = \begin{pmatrix} 0.392 & 0.111 & -0.006 \\ 0.111 & 0.584 & -0.005 \\ -0.006 & -0.005 & 0.024 \end{pmatrix}. \quad (53)$$

The matrix representation of the measured fourth-order orientation tensor \mathbb{N} in Voigt notation [60] (non-normalized, see, e.g., Cowin [61])

reads as follows

$$N_{ijkl} = \begin{pmatrix} 0.2780 & 0.1060 & 0.0080 & -0.0007 & -0.0049 & 0.0474 \\ 0.1060 & 0.4680 & 0.0100 & -0.0035 & -0.0007 & 0.0622 \\ 0.0080 & 0.0100 & 0.0060 & -0.0007 & 0.0000 & 0.0014 \\ -0.0007 & -0.0035 & -0.0007 & 0.0100 & 0.0015 & -0.0010 \\ -0.0049 & -0.0007 & 0.0000 & 0.0015 & 0.0080 & -0.0010 \\ 0.0474 & 0.0622 & 0.0014 & -0.0010 & -0.0010 & 0.1060 \end{pmatrix}. \quad (54)$$

It should be noted that \mathbb{N} given in Eq. (54) has to be transferred to the normalized Voigt notation [62] first in order to apply tensor operations. In addition, the SQC proposed by Karl et al. [12] for estimating the effective anisotropic behavior reads

$$\mathbb{F}(\mathbb{N}) = \frac{\text{sym}(\mathbb{N} \otimes \mathbb{N})}{\frac{1}{3}(1 + 2\|\mathbb{N}\|^2)}, \quad (55)$$

whereas all other closures listed in Section 5.1 remain unchanged. In general, the matrix representation of the fourth-order orientation tensor \mathbb{N} is based on proposing the complete index symmetry first and then approximating the components depending on the closure in use. For details, the reader is referred to Karl et al. [12]. As the matrix material, polypropylene (PP) is considered with the Young’s modulus $E_M = 1.6$ GPa and Poisson’s ratio $\nu_M = 0.4$ [63]. Glass fibers serve as the reinforcement material with $E_F = 73$ GPa and $\nu_F = 0.22$ [63]. Both the matrix and the fibers are assumed to be isotropic with homogeneous elastic properties. Based on the data of Müller et al. [59], the mean fiber aspect ratio $\alpha \approx 26$ is used combined with the fiber volume fraction $c_F = 0.13$ (PP-GF30). For predicting the effective properties, the mean-field model of Mori and Tanaka [64] is used for both the effective stiffness tensor $\bar{\mathbb{C}}$ and the effective viscosity tensor $\bar{\mathbb{V}}$ [4,20,65–67]

$$\begin{aligned} \bar{\mathbb{C}} &= \mathbb{C}_M + c_F \left(c_F \delta \mathbb{C}^{-1} + c_M \left((\delta \mathbb{C}^{-1} + \mathbb{P}_{0,S})^{-1} \right)_F^{-1} \right)^{-1}, \\ \bar{\mathbb{V}} &= \mathbb{V}_M + \frac{c_F}{c_M} \langle \mathbb{P}_{0,V}^{-1} \rangle_F. \end{aligned} \quad (56)$$

In Eq. (56), the abbreviation $\delta \mathbb{C} = \mathbb{C}_F - \mathbb{C}_M$ is used with the index F indicating the fiber phase and M referring to the matrix phase,

³ Internal database, Institute of Engineering Mechanics - Chair for Continuum Mechanics, Karlsruhe Institute of Technology (KIT)

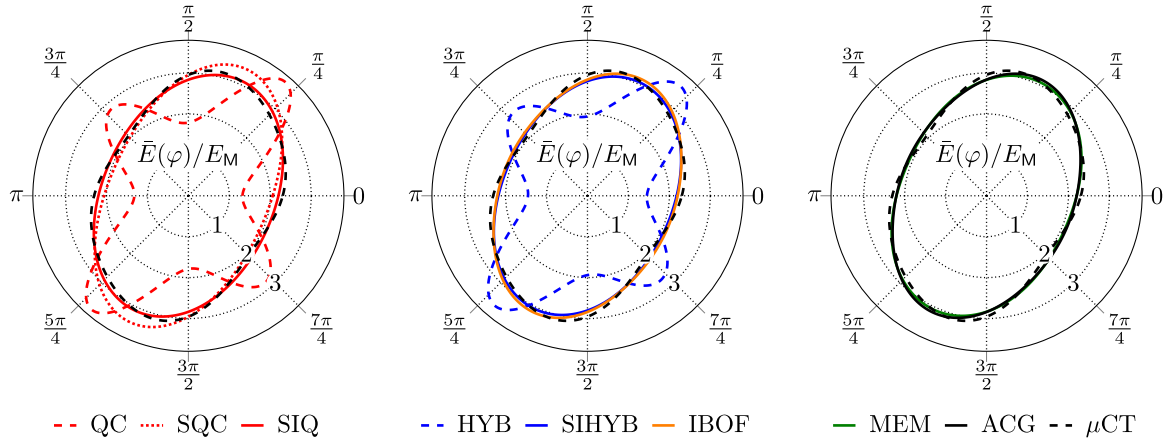


Fig. 4. Direction-dependent normalized effective Young's modulus $\bar{E}(\varphi)/E_M$ in the $e_1 - e_2$ -plane for the considered orientation state with respect to different closure approximations.

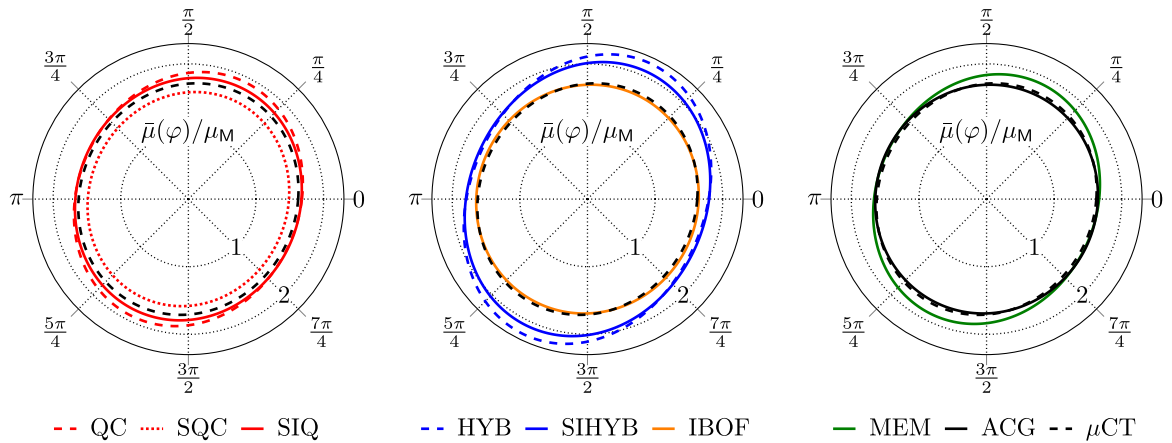


Fig. 5. Direction-dependent normalized effective shear viscosity $\bar{\mu}(\varphi)/\mu_M$ in the $e_1 - e_2$ -plane for the considered orientation state with respect to different closure approximations.

respectively. The polarization tensor for the solid [68] is denoted by $\mathbb{P}_{0,S}$ and the incompressible representation for the fiber suspension [4] reads as $\mathbb{P}_{0,V}$, respectively. To account for the fiber orientation state, the operator $\langle \cdot \rangle_F$ refers to the orientation averaging procedure introduced by Advani and Tucker [2]. The results presented in this section are based on the following scalar representation of the effective directional Young's modulus \bar{E} and the direction-dependent shear viscosity $\bar{\mu}$ [4, 62,67]

$$\frac{1}{\bar{E}(\mathbf{d})} = \mathbf{d} \otimes \mathbf{d} \cdot \bar{\mathbb{C}}^{-1}[\mathbf{d} \otimes \mathbf{d}],$$

$$\frac{1}{2\bar{\mu}(\mathbf{d}, \mathbf{p})} = \sqrt{2} \text{sym}(\mathbf{d} \otimes \mathbf{p}) \cdot \bar{\mathbb{V}}^{-1}[\sqrt{2} \text{sym}(\mathbf{d} \otimes \mathbf{p})]. \quad (57)$$

In Eq. (57), the tensile or the shear direction is indicated by \mathbf{d} and \mathbf{p} stands for normal vector of the shear plane. Within this study, both $\bar{E}(\mathbf{d})$ and $\bar{\mu}(\mathbf{d}, \mathbf{p})$ are restricted to the $e_1 - e_2$ -plane with $\mathbf{p} = e_3$. As a consequence, the argument list of \bar{E} and $\bar{\mu}$ is reduced to an angle $\varphi \in [0, 2\pi)$. Please note that Eq. (57) only represents the instantaneous anisotropic viscosity and any reorientation of the fibers is not considered [4,12]. Further information about the basic assumptions of mean-field homogenization and the unified homogenization of viscous fiber suspensions and solid fiber reinforced composites are given in Karl and Böhlke [4] and the references therein.

In Fig. 4, the direction-dependent normalized effective Young's modulus $\bar{E}(\varphi)/E_M$ is shown for all considered closure approximations. By comparing the closure-related results with the stiffness prediction based on the exact fourth-order orientation tensor (μCT), the predictive capabilities of the closures can be assessed. In the following, the μCT -curve is assumed to represent the exact result. The anisotropic elastic

behavior is not predicted well by both QC [12] and HYB based on the missing total index symmetry of the respective closure function. As already shown by Karl et al. [12] the SQC improves the QC-related results significantly, but the IBOF closure still achieves a better approximation of the real anisotropic stiffness. In contrast, the proposed implicit closures SIQ and SIHYB deviate only slightly from the IBOF closure, which in turn approximates the ACG closure. As in the previous Section 5.1, it is observed that both implicit closures are capable of substituting the MEM closure.

In Fig. 5, the direction-dependent normalized effective shear viscosity $\bar{\mu}(\varphi)/\mu_M$ is shown for all considered closure approximations. In particular, the performance of different closure approximations within anisotropic viscosity models is important in the context of flow-fiber coupled mold-filling simulation. Further details about flow-fiber coupling are provided in recent publications, e.g., [50,69–75]. Compared to Fig. 4, the proposed implicit closures deviate more from μCT , IBOF and ACG regarding the viscous anisotropy. Both IBOF and ACG predict the effective viscosity accurately based on the prediction with the measured orientation tensor in use. It is observed that both implicit closures improve the prediction compared to their explicit formulation. In case of QC and HYB, no anisotropy errors related to the violated full index symmetry of both closures are present. Using QC leads to a small overestimation, whereas HYB predicts the highest effective viscosity. SQC leads to a slight underestimation and SIQ lies between QC and SQC. In view of approximating the results of the MEM closure, SIQ is more suitable than SIHYB in case of anisotropic viscosity. In addition, SIQ is evaluated more accurately with respect to SIHYB.

Table 1
Absolute computation time t_c and approximate relative computation time t_{rel} for all considered closure approximations.

Closure	t_c in s	t_{rel} in %
MEM	0.31688170	486024
ACG	0.11489970	176230
SIHYB	0.00011718	180
SIQ	0.00007490	115
IBOF	0.00006520	100
HYB	0.00001681	26
SQC	0.00000697	11
QC	0.00000186	3

5.3. Computational effort

Finally, to evaluate the numerical effort of the different closures, the absolute computation time t_c needed to approximate the fourth-order fiber orientation tensor \mathbb{N} for a specific closure is measured relative to the computation time of the IBOF closure t_c^{IBOF} . With both measures at hand, the relative computation time t_{rel} is defined as follows

$$t_{rel} = \frac{t_c}{t_c^{IBOF}}. \quad (58)$$

In the case of orientation evolution, the data refer to the effort in each temporal integration step, whereas for the prediction of anisotropic properties the fourth-order fiber orientation tensor \mathbb{N} only needs to be calculated once. Table 1 lists the timings recorded on a Lenovo ThinkPad X1 Yoga with Intel® Core™ i7-10510U CPU (1.80 GHz) and 16 GB RAM using Matlab®. As previously reported, 5810 integration points on the unit sphere are used for MEM and ACG, the tolerance is fixed to 10^{-8} and the initial guess of Newton's method for SIQ and SIHYB is $s_0 = 0.25$. The results show that the highest numerical effort is required by MEM followed by ACG. The closures HYB, SQC and QC come with the least effort. In addition, the computational efforts for IBOF and the new closures SIQ and SIHYB are on the same order of magnitude. It is noted that no runtime-optimized implementation of MEM [76] and ACG [14,15] is used.

6. Summary and conclusion

In the present manuscript a novel implicit closure approach is proposed based on the contraction condition $\mathbb{N}[I] = \mathbb{N}$ involving orientation tensors of the first kind [1,2]. By considering fully symmetric approximations, additional requirements are fulfilled, namely the trace condition and the consistency with the flow in view of the trace-preserving property of the Folgar–Tucker equation [2,16]. Two fully symmetric implicit closures are investigated representing an innovative class of closure approaches, namely the symmetric implicit quadratic closure (SIQ) and the symmetric implicit hybrid closure (SIHYB). The SIQ closure approach extends the symmetric quadratic closure (SQC) proposed by Karl et al. [12] and SIHYB combines both approaches in view of the classical hybrid closure [2,8]. The present analysis shows that SIQ represents a realizable closure meaning that it is based on an orientation distribution function. In contrast, the SIHYB approach is not based on an orientation distribution function in general, since the linear part represents a non-realizable closure [24]. Both proposed implicit closures are able to exactly recover the correct fourth-order orientation tensor for the unidirectional, isotropic and planar isotropic case. In the context of fiber orientation evolution within a simple shear flow and the prediction of the effective viscous and elastic anisotropy for a given orientation state, SIQ and SIHYB are compared with well-known closure schemes. In the following, the results are summarized and the related conclusions are drawn:

- In case of orientation evolution, the SIQ and SIHYB closures show oscillatory behavior, closely following the maximum entropy closure (MEM) [31–35] over the entire considered range of the fiber interaction parameter C_1 . The SIHYB approach is capable of approximating the MEM results with respect to lower computational cost. Of course, MEM is able to be extended to known higher order orientation tensors improving the approximation, which is not possible for SIHYB. In contrast to the estimation of the effective stiffness, the fiber orientation evolution is not well-approximated compared to IBOF and ACG, even for typical values of the fiber interaction parameter C_1 in the interval $[5 \cdot 10^{-4}, 5 \cdot 10^{-3}]$. Likewise, the accuracy of SIQ and SIHYB compared to the solution of the Fokker–Planck equation is rated as insufficient. In addition, the oscillations of SIQ and SIHYB also occur within the more relevant RSC [53] and ARD [54] models. This allows the conclusion that the implicit approaches in a non-stabilized formulation should not be used in engineering practice.
- The MEM-approximating property of the proposed SIQ and SIHYB closures originates from an approximation of the lowest order MEM-formulation recently published by Papenfuss [36].
- For estimating the effective stiffness with different closure approaches, the computational experiments demonstrate that the implicit closures strongly improve the results with respect to their explicit formulation. Both SIQ and SIHYB are capable of approximating the MEM prediction and the results lie close to the IBOF and ACG. Overall, there is a rather good agreement with the prediction of effective stiffness based on the measured fourth-order tensor, which is considered accurate.
- Provided that all necessary algebraic conditions are satisfied by the closure (excluding QC and HYB), the anisotropy plots of Figs. 4 and 5 look similar for all applied closures. The considered common closures and the new approaches SIQ and SIHYB depend on the intrinsically orthotropic second-order fiber orientation tensor and this implies the orthotropic symmetry of the closed fourth-order orientation tensor. Therefore, the maximal class of anisotropy predicted by the new closure approach is orthotropy. This issue is discussed in the recent publications of Bauer and Böhlke [28] and of Tucker [27]. Conversely, this apparent restriction means that the quality of standard closures depending on the second-order fiber orientation tensor should not be judged solely on the basis of estimating the effective properties. In order to comprehend the quality of closures holistically, the behavior with regard to the prediction of the fiber orientation evolution in flow simulations must also be examined. A closure that is suitable for engineering practice is characterized by the fact that both the effective properties and the orientation evolution are predicted accurately.
- Analogously, the implicit closures strongly improve the predictions of the effective viscosity. However, the difference between the implicit closures and IBOF/ACG is more distinct in the case of anisotropic linear elastic properties. In this context, SIQ is capable of approximating the MEM results and an overall good agreement of SIQ with the measured data is observed.
- Since both SIQ and SIHYB can be reduced to a one-dimensional Newton's method, these closures are simple to compute and represent accurate approximations with respect to anisotropic property predictions.

CRedit authorship contribution statement

Tobias Karl: Conceptualization (lead), Methodology, Formal analysis (lead), Investigation, Software, Data curation, Visualization, Writing – original draft, writing – review & editing. **Matti Schneider:** Conceptualization, Formal analysis, Discussion, Funding acquisition, Writing – review & editing. **Thomas Böhlke:** Supervision, Discussion, Funding acquisition, Writing – review & editing. All authors read and approved the manuscript.

Declaration of competing interest

The authors declare that they have no known competing financial interests or personal relationships that could have appeared to influence the work reported in this paper.

Data availability

Data will be made available on request.

Acknowledgments

The partial financial support by the Friedrich und Elisabeth Boysen-Stiftung (Grant BOY-163) is gratefully acknowledged by TK and TB. MS gratefully acknowledges the support by the Deutsche Forschungsgemeinschaft (DFG, German Research Foundation) - 255730231. MS received partial support by the European Research Council within the Horizon Europe program - project 101040238. The authors thank the anonymous reviewers for their insightful comments and suggestions.

Appendix A. One-dimensional formulation of SIHYB

Analogous to the SIQ closure, the SIHYB closure can also be formulated one-dimensionally, which allows the simple application of Newton’s method. The closure function $\mathbb{F}(\mathbf{B})$ and the corresponding function $\mathbf{F}(\mathbf{B})$ whose roots \mathbf{B} are sought read as follows according to Eqs. (35) and (36) with $k = 1 - 27\det(\mathbf{N})$

$$\begin{aligned} \mathbb{F}(\mathbf{B}) &= (1 - k) \left(-\frac{3}{35} \text{sym}(\mathbf{I} \otimes \mathbf{I}) + \frac{6}{7} \text{sym}(\mathbf{I} \otimes \mathbf{B}) \right) + k \text{sym}(\mathbf{B} \otimes \mathbf{B}), \\ \mathbf{F}(\mathbf{B}) &= \frac{1 - k}{7} (\text{tr}(\mathbf{B}) - 1) \mathbf{I} + \left(1 - k + \frac{k}{3} \text{tr}(\mathbf{B}) \right) \mathbf{B} + \frac{2k}{3} \mathbf{B}^2 - \mathbf{N}. \end{aligned} \tag{A.1}$$

By using the results already discussed in Section 4.2, the isotropic state ($k = 0$) leads to the linear Eq. (37) having the unique solution $\mathbf{B} = \mathbf{N} = \mathbf{I}/3$. For the unidirectional state ($k = 1$) the SIHYB closure reduces to the SIQ closure whose unique solution $\mathbf{B} = \mathbf{N} = \mathbf{e}_1 \otimes \mathbf{e}_1$ follows from the discussion in Section 3.4.

For orientation-dependent parameter values $k \in (0, 1)$ the one-dimensional formulation of the SIHYB closure is derived as follows. By using both $s = \text{tr}(\mathbf{B})/4$ analogous to SIQ and $\mathbf{F}(\mathbf{B}) = \mathbf{0}$ one can write Eq. (A.1) in the following form with the abbreviations $a(s, k)$ and $b(s, k)$

$$\begin{aligned} \mathbf{0} &= \mathbf{B}^2 + a\mathbf{B} + b\mathbf{I} - \frac{3}{2k} \mathbf{N}, \\ a &= \frac{3 + (4s - 3)k}{2k}, \\ b &= \frac{3(1 - k)(4s - 1)}{14k}. \end{aligned} \tag{A.2}$$

Completing the square analogous to SIQ leads to

$$\mathbf{0} = \left(\mathbf{B} + \frac{a}{2} \mathbf{I} \right)^2 + \left(b - \frac{a^2}{4} \right) \mathbf{I} - \frac{3}{2k} \mathbf{N} \tag{A.3}$$

with the solution

$$\mathbf{B} = -\frac{a}{2} \mathbf{I} + \sqrt{\frac{3}{2k} \mathbf{N} + \left(\frac{a^2}{4} - b \right) \mathbf{I}}. \tag{A.4}$$

It should be noted that $\mathbf{BN} = \mathbf{NB}$ holds based on Eq. (A.2) which means that \mathbf{N} and \mathbf{B} commute and are thus jointly diagonalizable. By computing the trace of both sides of Eq. (A.4) on can derive the implicit equation for s

$$4s = -\frac{a}{2}d + \sum_{i=1}^d \sqrt{\frac{3\lambda_i}{2k} + \frac{a^2}{4} - b}. \tag{A.5}$$

Please note that a and b depend on s and $d = 2, 3$ represents the spatial dimension. The eigenvalues μ_i of \mathbf{B} can be computed with the solution s as follows

$$\mu_i = -\frac{a}{2} + \sqrt{\frac{3\lambda_i}{2k} + \frac{a^2}{4} - b}. \tag{A.6}$$

In order to apply one-dimensional Newton’s method, the following function $f(s)$ is defined

$$f(s) = 4s + \frac{a}{2}d - \sum_{i=1}^d \sqrt{\frac{3\lambda_i}{2k} + \frac{a^2}{4} - b} \tag{A.7}$$

with the corresponding derivative $f'(s)$ for $k \in (0, 1)$

$$f'(s) = 4 + \sum_{i=1}^d \left(1 - \frac{9(1 - k) + 28sk}{28k \sqrt{\frac{3\lambda_i}{2k} + \frac{a^2}{4} - b}} \right). \tag{A.8}$$

It is shown in the following that the function f is strongly monotone and $f'(s) \geq 4$ holds referring to

$$1 - \frac{9(1 - k) + 28sk}{28k \sqrt{\frac{3\lambda_i}{2k} + \frac{a^2}{4} - b}} \geq 0 \tag{A.9}$$

which is equal to

$$28k \sqrt{\frac{3\lambda_i}{2k} + \frac{a^2}{4} - b} \geq 9(1 - k) + 28sk. \tag{A.10}$$

Squaring both sides and using the definitions of $a(s, k)$ and $b(s, k)$ leads to the following condition which is independent of s

$$g(k) = 192k^2 + (1176\lambda_i - 552)k + 360 \geq 0, \tag{A.11}$$

with $\lambda_i \in [0, 1]$ and $k \in (0, 1)$. The lower bound $k \rightarrow 0$ leads to $360 \geq 0$ whereas the upper bound $k \rightarrow 1$ refers to $1176\lambda_i \geq 0$, $\lambda_i \in [0, 1]$. In general, the roots of the function g read

$$k_{1,2} = -\frac{49\lambda_i}{16} + \frac{23}{16} \pm \frac{7}{16} \sqrt{49\lambda_i^2 - 46\lambda_i + 1}. \tag{A.12}$$

The roots $k_{1,2}$ are real numbers only for $49\lambda_i^2 - 46\lambda_i + 1 \geq 0$ which is valid for

$$0 \leq \lambda_i \leq \frac{23}{49} - \frac{4\sqrt{30}}{49} \tag{A.13}$$

and

$$\frac{23}{49} + \frac{4\sqrt{30}}{49} \leq \lambda_i \leq 1. \tag{A.14}$$

For the above intervals of λ_i , $k_{1,2} \notin (0, 1)$ holds and Eq. (A.11) is valid. As a consequence, the function f is strongly monotone with $f'(s) \geq 4$. The sought root s of the function f can be computed using one-dimensional Newton’s method and \mathbf{B} is obtained via Eq. (A.6) and a back transformation into the spatial coordinate system using the eigenvectors of \mathbf{N} .

Appendix B. Supplementary material

Supplementary material related to this article can be found online at <https://doi.org/10.1016/j.jnnfm.2023.105049>.

References

- [1] K.-I. Kanatani, Distribution of directional data and fabric tensors, *Internat. J. Engrg. Sci.* 22 (2) (1984) 149–164, [http://dx.doi.org/10.1016/0020-7225\(84\)90090-9](http://dx.doi.org/10.1016/0020-7225(84)90090-9).
- [2] S.G. Advani, C.L. Tucker, The use of tensors to describe and predict fiber orientation in short fiber composites, *J. Rheol.* 31 (8) (1987) 751–784, <http://dx.doi.org/10.1122/1.549945>.
- [3] S. Kugler, A. Kech, C. Cruz, T. Osswald, Fiber orientation predictions - A review of existing models, *J. Compos. Sci.* 4 (2) (2020) <http://dx.doi.org/10.3390/jcs4020069>.
- [4] T. Karl, T. Böhlke, Unified mean-field modeling of viscous short-fiber suspensions and solid short-fiber reinforced composites, *Arch. Appl. Mech.* 92 (12) (2022) 3695–3727, <http://dx.doi.org/10.1007/s00419-022-02257-4>.
- [5] K. Breuer, M. Stommel, W. Korte, Analysis and evaluation of fiber orientation reconstruction methods, *J. Compos. Sci.* 3 (3) (2019) <http://dx.doi.org/10.3390/jcs3030067>.

- [6] A. Al-Qudsi, H. Çelik, J. Neuhaus, C. Hopmann, A comparative study between fiber orientation closure approximations and a new orthotropic closure, *Polym. Compos.* 43 (11) (2022) 7669–7700, <http://dx.doi.org/10.1002/pc.26896>.
- [7] G.L. Hand, A theory of anisotropic fluids, *J. Fluid Mech.* 13 (1) (1962) 33–46, <http://dx.doi.org/10.1017/S0022112062000476>.
- [8] S.G. Advani, C.L. Tucker, Closure approximations for three-dimensional structure tensors, *J. Rheol.* 34 (3) (1990) 367–386, <http://dx.doi.org/10.1122/1.550133>.
- [9] M. Doi, Molecular dynamics and rheological properties of concentrated solutions of rodlike polymers in isotropic and liquid crystalline phases, *J. Polym. Sci.: Polym. Phys. Ed.* 19 (2) (1981) 229–243, <http://dx.doi.org/10.1002/pol.1981.180190205>.
- [10] K.-H. Han, Y.-T. Im, Modified hybrid closure approximation for prediction of flow-induced fiber orientation, *J. Rheol.* 43 (3) (1999) 569–589, <http://dx.doi.org/10.1122/1.551002>.
- [11] C. Petty, S. Parks, S. Shao, Flow-induced alignment of fibers, in: *Proceedings of 12th International Conference on Composite Materials ICCM-12*, Paris, 1999, URL <https://www.iccm-central.org/Proceedings/ICCM12proceedings/site/htmlpap/pap339.htm>.
- [12] T. Karl, D. Gatti, B. Frohnapfel, T. Böhlke, Asymptotic fiber orientation states of the quadratically closed Folgar-Tucker equation and a subsequent closure improvement, *J. Rheol.* 65 (5) (2021) 999–1022, <http://dx.doi.org/10.1122/8.0000245>.
- [13] D.E. Tyler, Statistical analysis for the angular central Gaussian distribution on the sphere, *Biometrika* 74 (3) (1987) 579–589, <http://dx.doi.org/10.2307/2336697>.
- [14] S. Montgomery-Smith, W. He, D.A. Jack, D.E. Smith, Exact tensor closures for the three-dimensional Jeffery's equation, *J. Fluid Mech.* 680 (2011) 321–335, <http://dx.doi.org/10.1017/jfm.2011.165>.
- [15] S. Montgomery-Smith, D. Jack, D.E. Smith, The fast exact closure for Jeffery's equation with diffusion, *J. Non-Newton. Fluid Mech.* 166 (7) (2011) 343–353, <http://dx.doi.org/10.1016/j.jnnfm.2010.12.010>.
- [16] F. Folgar, C.L. Tucker, Orientation behavior of fibers in concentrated suspensions, *J. Reinf. Plast. Compos.* 3 (2) (1984) 98–119, <http://dx.doi.org/10.1177/073168448400300201>.
- [17] M. Schneider, The sequential addition and migration method to generate representative volume elements for the homogenization of short fiber reinforced plastics, *Comput. Mech.* 59 (2) (2017) 247–263, <http://dx.doi.org/10.1007/s00466-016-1350-7>.
- [18] M. Schneider, An algorithm for generating microstructures of fiber-reinforced composites with long fibers, *Internat. J. Numer. Methods Engrg.* 123 (24) (2022) 6197–6219, <http://dx.doi.org/10.1002/nme.7110>.
- [19] J. Köbler, M. Schneider, F. Ospald, H. Andrä, R. Müller, Fiber orientation interpolation for the multiscale analysis of short fiber reinforced composite parts, *Comput. Mech.* 61 (6) (2018) 729–750, <http://dx.doi.org/10.1007/s00466-017-1478-0>.
- [20] R. Bertóti, D. Wicht, A. Hrymak, M. Schneider, T. Böhlke, A computational investigation of the effective viscosity of short-fiber reinforced thermoplastics by an FFT-based method, *Eur. J. Mech. B/Fluids* 90 (2021) 99–113, <http://dx.doi.org/10.1016/j.euromechflu.2021.08.004>.
- [21] N. Goldberg, F. Ospald, M. Schneider, A fiber orientation-adapted integration scheme for computing the hyperelastic Tucker average for short fiber reinforced composites, *Comput. Mech.* 60 (4) (2017) 595–611, <http://dx.doi.org/10.1007/s00466-017-1425-0>.
- [22] M. Nabergoj, J. Urevc, M. Halilović, Function-based reconstruction of the fiber orientation distribution function of short-fiber-reinforced polymers, *J. Rheol.* 66 (1) (2022) 147–160, <http://dx.doi.org/10.1122/8.0000358>.
- [23] W. Ogierman, Novel closure approximation for prediction of the effective elastic properties of composites with discontinuous reinforcement, *Compos. Struct.* 300 (2022) 116146, <http://dx.doi.org/10.1016/j.compstruct.2022.116146>.
- [24] J.K. Bauer, T. Böhlke, Variety of fiber orientation tensors, *Math. Mech. Solids* 27 (7) (2022) 1185–1211, <http://dx.doi.org/10.1177/10812865211057602>.
- [25] J.S. Cintra, C.L. Tucker, Orthotropic closure approximations for flow-induced fiber orientation, *J. Rheol.* 39 (6) (1995) 1095–1122, <http://dx.doi.org/10.1122/1.550630>.
- [26] D.H. Chung, T.H. Kwon, Invariant-based optimal fitting closure approximation for the numerical prediction of flow-induced fiber orientation, *J. Rheol.* 46 (1) (2002) 169–194, <http://dx.doi.org/10.1122/1.1423312>.
- [27] C.L. Tucker III, Planar fiber orientation: Jeffery, non-orthotropic closures, and reconstructing distribution functions, *J. Non-Newton. Fluid Mech.* 310 (2022) 104939, <http://dx.doi.org/10.1016/j.jnnfm.2022.104939>.
- [28] J.K. Bauer, T. Böhlke, On the dependence of orientation averaging mean field homogenization on planar fourth-order fiber orientation tensors, *Mech. Mater.* 170 (2022) 104307, <http://dx.doi.org/10.1016/j.mechmat.2022.104307>.
- [29] J.K. Bauer, M. Schneider, T. Böhlke, On the phase space of fourth-order fiber-orientation tensors, *J. Elasticity* 153 (2) (2023) 161–184, <http://dx.doi.org/10.1007/s10659-022-09977-2>.
- [30] M. Moakher, P.J. Basser, Fiber orientation distribution functions and orientation tensors for different material symmetries, in: I. Hotz, T. Schultz (Eds.), *Visualization and Processing of Higher Order Descriptors for Multi-Valued Data*, Springer International Publishing, Cham, 2015, pp. 37–71, http://dx.doi.org/10.1007/978-3-319-15090-1_3.
- [31] E.T. Jaynes, Information theory and statistical mechanics, *Phys. Rev.* 106 (4) (1957) 620–630, <http://dx.doi.org/10.1103/PhysRev.106.620>.
- [32] C. Bingham, An antipodally symmetric distribution on the sphere, *Ann. Statist.* 2 (6) (1974) 1201–1225, <http://dx.doi.org/10.1214/aos/1176342874>.
- [33] C.V. Chaubal, L.G. Leal, A closure approximation for liquid-crystalline polymer models based on parametric density estimation, *J. Rheol.* 42 (1) (1998) 177–201, <http://dx.doi.org/10.1122/1.550887>.
- [34] M. van Gorp, Letter to the Editor: On the use of spherical tensors and the maximum entropy method to obtain closure for anisotropic liquids, *J. Rheol.* 42 (5) (1998) 1269–1271, <http://dx.doi.org/10.1122/1.550921>.
- [35] V. Müller, T. Böhlke, Prediction of effective elastic properties of fiber reinforced composites using fiber orientation tensors, *Compos. Sci. Technol.* 130 (2016) 36–45, <http://dx.doi.org/10.1016/j.compscitech.2016.04.009>.
- [36] C. Papenfuss, Maximum entropy closure relation for higher order alignment and orientation tensors compared to quadratic and hybrid closure, *J. Model. Simul. Mater.* 5 (1) (2022) 39–52, <http://dx.doi.org/10.21467/jmsm.5.1.39-52>.
- [37] V. Verleye, F. Dupret, Prediction of fiber orientation in complex injection molded parts, *Am. Soc. Mech. Eng. Dev. Non-Newtonian Flows* 175 (1993) 139–164.
- [38] A. Mehta, M. Schneider, A sequential addition and migration method for generating microstructures of short fibers with prescribed length distribution, *Comput. Mech.* 70 (4) (2022) 829–851, <http://dx.doi.org/10.1007/s00466-022-02201-x>.
- [39] V. Lebedev, D. Laikov, A quadrature formula for the sphere of the 131st algebraic order of accuracy, *Dokl. Math.* 59 (3) (1999) 477–481.
- [40] R. Parrish, getLebedevSphere. MATLAB® Central File Exchange. Retrieved July 6, 2021, 2021, <https://www.mathworks.com/matlabcentral/fileexchange/27097-getlebedevsphere>.
- [41] P. Deuflhard, F. Bornemann, *Numerische Mathematik 2 - Gewöhnliche Differentialgleichungen*, third ed., De Gruyter, Berlin, New York, 2008, <http://dx.doi.org/10.1515/9783110203578>.
- [42] A.D. Fokker, Die mittlere Energie rotierender elektrischer Dipole im Strahlungsfeld, *Ann. Phys.* 348 (5) (1914) 810–820, <http://dx.doi.org/10.1002/andp.19143480507>.
- [43] C. Lohmann, Efficient algorithms for constraining orientation tensors in Galerkin methods for the Fokker-Planck equation, *Comput. Math. Appl.* 71 (5) (2016) 1059–1073, <http://dx.doi.org/10.1016/j.camwa.2016.01.012>.
- [44] C.L. Tucker III, Fiber Orientation Tools (v1.0.0). Retrieved February 10, 2023, 2021, <https://github.com/charlestucker3/Fiber-Orientation-Tools>.
- [45] M.C. Altan, L. Tang, Orientation tensors in simple flows of dilute suspensions of non-Brownian rigid ellipsoids, comparison of analytical and approximate solutions, *Rheol. Acta* 32 (3) (1993) 227–244, <http://dx.doi.org/10.1007/BF00434187>.
- [46] G.B. Jeffery, The motion of ellipsoidal particles immersed in a viscous fluid, *Proc. R. Soc. Lond. Ser. A* 102 (715) (1922) 161–179, <http://dx.doi.org/10.1098/rspa.1922.0078>.
- [47] M.S. Ingber, L.A. Mondy, A numerical study of three-dimensional Jeffery orbits in shear flow, *J. Rheol.* 38 (6) (1994) 1829–1843, <http://dx.doi.org/10.1122/1.550604>.
- [48] M. Junk, R. Illner, A new derivation of Jeffery's equation, *J. Math. Fluid Mech.* 9 (4) (2007) 455–488, <http://dx.doi.org/10.1007/s00021-005-0208-0>.
- [49] D. Mezi, G. Ausias, S.G. Advani, J. Férec, Fiber suspension in 2D nonhomogeneous flow: The effects of flow/fiber coupling for Newtonian and power-law suspending fluids, *J. Rheol.* 63 (3) (2019) 405–418, <http://dx.doi.org/10.1122/1.5081016>.
- [50] J. Férec, D. Mezi, S.G. Advani, G. Ausias, Axisymmetric flow simulations of fiber suspensions as described by 3D probability distribution function, *J. Non-Newton. Fluid Mech.* 284 (2020) 104367, <http://dx.doi.org/10.1016/j.jnnfm.2020.104367>.
- [51] R.S. Bay, Fiber Orientation in Injection Molded Composites: A Comparison of Theory and Experiment (Doctoral thesis), University of Illinois at Urbana-Champaign, 1991, <https://hdl.handle.net/2142/22217>.
- [52] N. Phan-Thien, X.-J. Fan, R. Tanner, R. Zheng, Folgar-Tucker constant for a fibre suspension in a Newtonian fluid, *J. Non-Newton. Fluid Mech.* 103 (2–3) (2002) 251–260, [http://dx.doi.org/10.1016/S0377-0257\(02\)00006-X](http://dx.doi.org/10.1016/S0377-0257(02)00006-X).
- [53] J. Wang, J.F. O'Gara, C.L. Tucker III, An objective model for slow orientation kinetics in concentrated fiber suspensions: Theory and rheological evidence, *J. Rheol.* 52 (5) (2008) 1179–1200, <http://dx.doi.org/10.1122/1.2946437>.
- [54] J.H. Phelps, C.L. Tucker III, An anisotropic rotary diffusion model for fiber orientation in short- and long-fiber thermoplastics, *J. Non-Newton. Fluid Mech.* 156 (3) (2009) 165–176, <http://dx.doi.org/10.1016/j.jnnfm.2008.08.002>.
- [55] J. Feng, C.V. Chaubal, L.G. Leal, Closure approximations for the Doi theory: Which to use in simulating complex flows of liquid-crystalline polymers? *J. Rheol.* 42 (5) (1998) 1095–1119, <http://dx.doi.org/10.1122/1.550920>.
- [56] S. Montgomery-Smith, Perturbations of the coupled Jeffery–Stokes equations, *J. Fluid Mech.* 681 (2011) 622–638, <http://dx.doi.org/10.1017/jfm.2011.237>.
- [57] S. Montgomery-Smith, Perturbations of the coupled Jeffery–Stokes equations – Corrigendum, 2011, <https://stephenmontgomerysmith.github.io/preprints/jeff-stokes-corrigendum.pdf>.
- [58] S. Montgomery-Smith, Non-linear instability of periodic orbits of suspensions of thin fibers in fluids, *J. Non-Newton. Fluid Mech.* 313 (2023) 105001, <http://dx.doi.org/10.1016/j.jnnfm.2023.105001>.

- [59] V. Müller, B. Brylka, F. Dillenberger, R. Glöckner, S. Kolling, T. Böhlke, Homogenization of elastic properties of short-fiber reinforced composites based on measured microstructure data, *J. Compos. Mater.* 50 (3) (2016) 297–312, <http://dx.doi.org/10.1177/0021998315574314>.
- [60] W. Voigt, *Lehrbuch der Kristallphysik*, B.G. Teubner, Leipzig, 1910.
- [61] S.C. Cowin, Properties of the anisotropic elasticity tensor, *Quart. J. Mech. Appl. Math.* 42 (2) (1989) 249–266, <http://dx.doi.org/10.1093/qjmam/42.2.249>.
- [62] T. Böhlke, C. Brüggemann, Graphical representation of the generalized Hooke's law, *Tech. Mech.* 21 (2) (2001) 145–158, URL <https://journals.ub.uni-magdeburg.de/ubjournals/index.php/techmech/article/view/1045>.
- [63] H. Schürmann, *Konstruieren Mit Faser-Kunststoff-Verbunden*, second ed., Springer, Berlin, Heidelberg, 2007, <http://dx.doi.org/10.1007/978-3-540-72190-1>.
- [64] T. Mori, K. Tanaka, Average stress in matrix and average elastic energy of materials with misfitting inclusions, *Acta Metall.* 21 (5) (1973) 571–574, [http://dx.doi.org/10.1016/0001-6160\(73\)90064-3](http://dx.doi.org/10.1016/0001-6160(73)90064-3).
- [65] B. Brylka, *Charakterisierung und Modellierung der Steifigkeit von langfaserverstärktem Polypropylen* (Doctoral thesis), Schriftenreihe Kontinuumsmechanik im Maschinenbau Band 10. Karlsruher Institut für Technologie (KIT), 2017, <http://dx.doi.org/10.5445/KSP/1000070061>.
- [66] P.A. Hessman, F. Welschinger, K. Hornberger, T. Böhlke, On mean field homogenization schemes for short fiber reinforced composites: unified formulation, application and benchmark, *Int. J. Solids Struct.* 230–231 (2021) 111141, <http://dx.doi.org/10.1016/j.ijsolstr.2021.111141>.
- [67] R. Bertóti, T. Böhlke, Flow-induced anisotropic viscosity in short FRPs, *Mech. Adv. Mater. Modern Processes* 3 (1) (2017) <http://dx.doi.org/10.1186/s40759-016-0016-7>.
- [68] P. Ponte Castañeda, J. Willis, The effect of spatial distribution on the effective behavior of composite materials and cracked media, *J. Mech. Phys. Solids* 43 (12) (1995) 1919–1951, [http://dx.doi.org/10.1016/0022-5096\(95\)00058-Q](http://dx.doi.org/10.1016/0022-5096(95)00058-Q).
- [69] C.-T. Huang, C.-H. Lai, Investigation on the coupling effects between flow and fibers on fiber-reinforced plastic (FRP) injection parts, *Polymers* 12 (10) (2020) <http://dx.doi.org/10.3390/polym12102274>.
- [70] Z. Wang, D.E. Smith, A fully coupled simulation of planar deposition flow and fiber orientation in polymer composites additive manufacturing, *Materials* 14 (10) (2021) <http://dx.doi.org/10.3390/ma14102596>.
- [71] Z. Wang, D.E. Smith, Finite element modelling of fully-coupled flow/fiber-orientation effects in polymer composite deposition additive manufacturing nozzle-extrudate flow, *Composites B* 219 (2021) 108811, <http://dx.doi.org/10.1016/j.compositesb.2021.108811>.
- [72] T. Karl, D. Gatti, T. Böhlke, B. Frohnäpfel, Coupled simulation of flow-induced viscous and elastic anisotropy of short-fiber reinforced composites, *Acta Mech.* 232 (6) (2021) 2249–2268, <http://dx.doi.org/10.1007/s00707-020-02897-z>.
- [73] Z. Wang, Exploring the applicability of a simplified fully coupled flow/orientation algorithm developed for polymer composites extrusion deposition additive manufacturing, *Int. Polym. Process.* 37 (1) (2022) 106–119, <http://dx.doi.org/10.1515/ipp-2021-4186>.
- [74] S. Lee, D. Shin, G. Kim, W. Ji, Numerical model for compression molding process of hybridly laminated thermoplastic composites based on anisotropic rheology, *Composites C* 7 (2022) 100215, <http://dx.doi.org/10.1016/j.jcomc.2021.100215>.
- [75] T. Karl, J. Zartmann, S. Dalpke, D. Gatti, B. Frohnäpfel, T. Böhlke, Influence of flow–fiber coupling during mold-filling on the stress field in short-fiber reinforced composites, *Comput. Mech.* 71 (5) (2023) 991–1013, <http://dx.doi.org/10.1007/s00466-023-02277-z>.
- [76] Y. Luo, J. Xu, P. Zhang, A fast algorithm for the moments of Bingham distribution, *J. Sci. Comput.* 75 (3) (2018) 1337–1350, <http://dx.doi.org/10.1007/s10915-017-0589-2>.